Valorization of Kraft Lignin as Thickener in Castor Oil for Lubricant Applications

A. M. Borrero-López[1], F. J. Santiago-Medina[1], C. Valencia[1,2]*, M. E. Eugenio[3], R. Martin-Sampedro[3] and J. M. Franco[1,2]

[1]*Department of Chemical Engineering, University of Huelva, El Carmen Campus, Agrifood Campus of International Excellence (ceiA3), 21071 Huelva, Spain*
[2]*Pro²TecS – Chemical Process and Product Technology Research Center, University of Huelva, 21071 Huelva, Spain*
[3]*INIA-CIFOR, Ctra de la Coruña, km 7.5. 28040, Madrid, Spain*

ABSTRACT: It is known that large amounts of residual lignin are generated in the pulp and paper industry. A new alternative for Kraft lignin valorization, which consists of first a chemical modification using a diisocyanate and then the efficient dispersion in castor oil to achieve stable gel-like systems, is proposed in this work. Rheological properties and microstructure of these materials were determined by means of small amplitude oscillatory shear tests and viscous flow measurements and atomic force microscopy observations, respectively. Moreover, both standardized penetration tests and tribological assays, usually performed in the lubricant industry, were carried out to evaluate the performance characteristics as lubricating greases. Linear viscoelasticity functions are affected by the lignin/diisocyanate ratio and thickener concentration. The thermo-rheological response evidenced a softening temperature of around 105 °C. The microstructure of these gel-like dispersions is composed of interconnected thin fibers, homogeneously distributed in castor oil. Moreover, the NCO-functionalized lignin gel-like dispersions studied show lower friction coefficients than traditional lubricating greases.

KEYWORDS: Kraft lignin, diisocyanate, gel-like dispersion, rheology, thermal properties

1 INTRODUCTION

Lignin is nowadays considered the main aromatic renewable resource and an excellent alternative feedstock for the synthesis of value-added chemicals and polymers. Lignin extraction from lignocellulosic biomass (wood, annual plant, etc.) represents the key point to its large use for industrial applications [1]. It is the second most abundant renewable resource after cellulose [2] and mainly results from the polymerization of three monomers: p-coumaryl alcohol, coniferyl alcohol and synapyl alcohol. Each of these monolignols leads to different types of lignin units called p-hydroxyphenyl (H), guaiacyl (G) and syringyl (S), respectively. Although these monomers are the main precursors of lignin, it is well known that others can also participate in its formation, such as coniferaldehyde, acylated monolignols, etc. The resulting polymeric structure is a complex macromolecule, which contains a wide variety of functional groups and different types of bonds depending on biomass source [3]. Thus, hardwood lignin consists principally of G and S units and traces of H units, whereas softwood lignin mostly consists of G units, with low levels of H units [1]. Furthermore, not only the original source but also the method used to isolate the different lignins has an influence on their structural characteristics and, therefore, on their industrial applicability.

It is known that large amounts of residual lignin are generated in the pulp and paper industry. In the pulping manufacturing process, the lignin contained in the wood is dissolved in the process liquor, obtaining the so-called black liquor. In the case of the predominant Kraft pulping process, the black liquor is typically burned in order to obtain energy. Although previous structural modification processes are needed to increase lignin's initial poor properties, residual Kraft lignin may be otherwise used to obtain value-added products [4]. The abundance of the chemical sites in lignin structure offers different possibilities for chemical modifications. For instance, lignin has phenolic

hydroxyl groups and aliphatic hydroxyl groups at C-α and C-γ positions on the side chain. Phenolic hydroxyl groups are the most reactive functional groups and can significantly influence the chemical reactivity of the material. Among several polymerization methods with lignin macromonomers, lignin-based urethane polymerization has been investigated using different diisocyanates, reaction conditions and ratios of functionalities [5–7]. Moreover, lignin macromonomers have been incorporated into polycaprolactone, polyester [8], polyurethanes [6, 8–10], phenolics and urea matrices [11], or have been used to prepare and reinforce vegetable oil-based polyurethane composites [12–15].

On the other hand, there is a general tendency based on the use of natural components in a wide variety of products to promote both the replacement of non-renewable raw materials by renewable resources and the minimization of the environmental impact caused by industrial wastes [16–18]. Over the past two decades, a renewed interest in different vegetable oil-based lubricants has occurred as a result of environmental concerns. Vegetable oils with high viscosity indices, low volatility and high flash points have been employed in a series of applications over lubricants and additives in polymers, coatings and resins [19]. Moreover, a great number of research works dealing with the lubrication properties of different vegetable oils and some chemical derivatives have been reported in the past few years. Among them, castor oil is considered one of the most interesting alternative base oils, especially due to its high viscosity and good performance characteristics at low temperatures [20, 21]. Some adverse properties can be overcome by using some additives as previously reported [21, 22]. On the other hand, the replacement of traditional thickening agents in lubricating greases, such as lithium, calcium or aluminum soaps, by others derived from renewable resources, like some biopolymers, is a complicated task due to the technical efficiency of metallic soaps to impart the desired rheological, thermal and tribological properties to the bulk system. Previous research focused on the proper dispersion of different types of gelifiers, including some cellulose derivatives, in vegetable oils in order to achieve suitable gel-like characteristics and suitable lubricant performance have been reported [23–26]. In general, similar rheological and thermal characteristics to those displayed by traditional metallic soap-based greases were found but there are still some limitations regarding physical and mechanical stabilities. A significant improvement was achieved by performing the functionalization of cellulosic derivatives with isocyanate groups, which are also able to chemically interact with hydroxyl groups of castor oil, thus resulting in promising formulations

[27, 28]. Following this approach, the main objective of this work was to develop and characterize new gel-like formulations, potentially applicable as biodegradable lubricating greases, based on residual Kraft lignin once chemically modified with 1,6-hexamethylene diisocyanate and properly dispersed in castor oil.

2 MATERIALS AND METHODS

2.1 Materials

Eucalyptus globulus chips were supplied by a Spanish pulp mill (Factoría La Montañanesa, Torraspapel-Lecta Group). The 1,6-Hexamethylene diisocyanate (HMDI), purum grade (≥ 98.0%), was obtained from Sigma-Aldrich. Castor oil (Guinama, Spain) was selected as lubricant base oil to prepare gel-like dispersions. All other common reagents and solvents employed were purchased from Sigma-Aldrich.

A commercial model lithium lubricating grease (Castrol Optipit, Germany) and a semi-biodegradable one based on vegetable oil and a calcium thickener (kindly supplied by Verkol, Spain) were used as benchmarks.

2.2 Kraft Pulping

Kraft cooking of *Eucalyptus globulus* chips was performed in a 26 L batch reactor furnished with a system for recirculation and heating of the cooking liquor. Prior to cooking, the chips were steamed for 5 min to facilitate impregnation of chemicals. The cooking temperature was controlled by a computer run specially developed software. Applied cooking conditions were: 16% active alkali, 20% sulphidity, 4 L kg⁻¹ liquor/wood ratio, 170 °C cooking temperature, 60 min to reach cooking temperature and 30 min at cooking temperature. These conditions correspond to an H-factor of 460. The H-factor is a well-known control parameter in the pulping process that includes time and temperature as a single variable, which is calculated according to the following equation:

$$H = \int_0^t e^{\left(43.2 - \frac{16115}{T}\right)} dt$$

where T is the temperature (K) and t the cooking time (hours).

2.3 Lignin Precipitation

After Kraft pulping, lignin was precipitated from the black liquor by acidification adding sulphuric acid until pH 2.5 (initial pH was 13.2). Then, precipitated

lignin was air dried and milled for 20 min using a Retsch agate mortar grinder (model RMO).

2.4 Kraft Lignin Functionalization

All functionalization reactions were performed in round-bottom flasks where reactants were mixed. Toluene, employed as solvent in the reaction between the lignin powder and the diisocyanate, was purified according to standard literature techniques. The 1,6-hexamethylene diisocyanate (HMDI) was stored at 4 °C.

Functionalization of Kraft lignin (KL) was carried out according to methodologies previously reported [27] and by modifying the lignin/HMDI weight ratio. The KL was added to a round-bottom flask with toluene while stirring at room temperature, becoming a suspension. Then, triethylamine (Et$_3$N) and HMDI were also added to the system, the last one dropwisely. The solution was vigorously stirred at room temperature for 24 h. The synthesis was carried out under inert atmosphere of argon. Afterwards, the mixture was concentrated in a rotary evaporator, resulting in a black compound. The product was prepared immediately before being used. The different proportions of KL, HMDI, Et$_3$N and toluene used in the reaction as well as the yield are collected in Table 1.

2.5 Preparation of Gel-Like Dispersions

Gel-like dispersion samples were prepared in an open vessel, using a controlled rotational speed mixing device RW 20 (IKA), equipped with an anchor impeller to disperse the different functionalized lignin samples in the oil. NCO-functionalized lignin was slowly added to the castor oil at concentrations of 20% and 30% (w/w) under agitation (70 rpm). The mixing process was maintained for 24 h at room temperature. Finally, the resulting dispersion was homogenized with an Ultra-Turrax T50 basic (IKA) rotor-stator turbine at 4000 rpm for 1 min. Batches of 50 g were prepared for each formulation investigated.

2.6 Characterizations

2.6.1 Precipitated Lignin Composition

The composition of the precipitated lignin was determined by standard analytical methods (National Renewable Energy Laboratory NREL/TP-510-42618). The sample was subjected to quantitative acid hydrolysis in two steps to determine the carbohydrate composition. The hydrolyzed liquid obtained was then analyzed for sugar content using an Agilent Technologies 1260 HPLC fitted with a refractive index detector and an Agilent Hi-Plex Pb column operated at 70 °C with Milli-Q water as mobile phase pumped at a rate of 0.6 mL. The solid residue remaining after the acid hydrolysis is considered acid-insoluble lignin (Klason lignin). Moreover, ash was also determined following the standard UNE 57050:2003.

2.6.2 Thermogravimetric Analysis (TGA)

Measurements of mass losses versus temperature were carried out by using a thermogravimetric analyzer, model Q-50 (TA Instrument Waters, USA) under N$_2$ purge. Typically, 5–10 mg of sample were placed on a platinum pan and heated from 30 to 600 °C at 10 °C/min.

2.6.3 Fourier Transform Infrared (FTIR) Spectroscopy

Fourier transform infrared spectroscopy spectra were obtained with a JASCO FT/IR-4200 (Jasco Inc., Japan) apparatus. A small drop of functionalized lignin or gel-like dispersion samples was placed between two KBr disks (32 × 3 mm). Then, the set was placed into an appropriate sample holder. The spectra were obtained in a wavenumber range of 400–4000 cm^{-1}, at 4 cm^{-1} resolution, in the transmission mode.

2.6.4 Rheological Characterization of Gel-Like Dispersions

Gel-like NCO-functionalized lignin-based dispersions were rheologically characterized in both

Table 1 Proportions of Kraft lignin (KL), hexamethylene diisocyanate (HMDI), triethylamine (Et$_3$N) and toluene used in the functionalization reaction and yield obtained.

Thickener code	Lignin (g)	HMDI (g)	Et$_3$N (g)	Toluene (ml)	Yield (%)
KL1	10	10	20	100	85
KL2	10	20	20	100	91
KL4	10	40	20	150	92

controlled-stress (HAAKE RheoScope, Thermo Fisher Scientific, Germany) and controlled-strain (ARES, Rheometric Scientific, UK) rheometers, using serrated plate-plate (20 and 25 mm diameter respectively, 1 mm gap) geometries. Small amplitude oscillatory shear (SAOS) tests were carried out inside the linear viscoelastic region in a frequency range of 0.03–100 rad/s at 25 °C. Stress sweep tests were previously performed to determine the linear viscoelastic regime. Measurements were done one day, one week, one month and four months after gel-like dispersion preparation. The SAOS tests were obtained at different temperatures carried out between 30 and 155 °C. Apparent viscosity was determined by applying a stepped shear rate ramp in a shear rate range of 10^{-2}–10^{2} s^{-1}, using plate-plate geometry (25 mm) with grooved surfaces to overcome the wall slip phenomena usually observed in lubricating greases [29]. At least two replicates of each test were carried out on fresh samples.

2.6.5   *Penetration and Tribological Tests*

Unworked penetration indexes were determined according to the ASTM D1403 standard, by using a Seta Universal penetrometer model 17000-2 with one-quarter cone geometry (Stanhope-Seta, UK). The one-quarter scale penetration values were converted into the equivalent full-scale cone penetration values, following the ASTM D217 standard. Classical consistency NLGI grade was established according to these penetration values [30]. At least three replicates of penetration measurements were done.

Tribological tests were performed in a tribology measuring cell coupled with a Physica MCR-501 rheometer. The tribological cell deals with a 1/2″ diameter steel ball (1.4301 grade 100) rotating on three 45° inclined steel plates (1.4301). The stationary friction coefficient was obtained by applying a normal force of 20 N, resulting in a maximum contact Hertzian pressure of ~1.72 GPa and setting a constant rotational speed of 10 rpm for 10 min. At least five replicates of each test were done on fresh samples at room temperature. For the sake of comparison, tribological tests were also carried out under the same conditions on two commercial lubricating greases, typical lithium grease (Castrol Optipit, Germany) and one based on vegetable oil and calcium thickener (Verkol, Spain).

2.6.6   *Atomic Force Microscopy (AFM) Observations*

Morphological observation of a selected gel-like dispersion sample was investigated with a multimode AFM connected to a Nanoscope IV scanning probe microscope controller (Digital Instruments, Veeco

Metrology Group Inc., Santa Barbara, CA) using the tapping mode with phase detection imaging at room temperature. The amplitude of oscillation typically ranges from 20 nm to 100 nm. The tip lightly interacts with the sample surface during scanning, providing high-resolution images with minimum sample damage. Silicon Nanosensors TM PPP-NCH AFM probes for tapping mode with a force constant of 42 N m^{-1} and resonance frequency of 330 kHz were used. Scan speed and windows were set at 1 Hz and 6 and 1 μm, respectively.

3   RESULTS AND DISCUSSION

3.1   Composition of Kraft Lignin

The Kraft lignin (KL) contains 4.98% carbohydrates (0.49% glucose, 4.29% xylose and 0.20% arabinose), which can probably be attributed to both LCCs (lignin carbohydrates bound) and non-bounded sugars. As can be observed, the predominant elemental sugar was xylose. These results are in concordance with those found by Dos Santos *et al.* [31] and Alekhina *et al.* [32]. The latter authors explained that this fact could be due to a combination of two factors, i.e., the low solubility in acid media of the hemicellulose (xylose) and the fast degradation of the cellulose into its monomers during the cooking process and then its further decomposition into degradation products.

The acid-insoluble lignin (Klason lignin) and the acid-soluble lignin (ASL) found in the precipitated lignin were 35.96% and 8.85%, respectively (44.81% total lignin). These results are also in concordance with those found by Alekhina *et al.* [32] when they precipitated the lignin at pH 2.5 (46.90% and 10.78% of Klason lignin and ASL, respectively). However, Dos Santos *et al.* [31] found a lower amount of ASL (1.60%) with a similar value of Klason lignin (40.93%). Yasuda *et al.* [33] studied the structure and formation mechanism of ASL and concluded that it is composed of low-molecular-weight degradation products and hydrophilic derivatives of lignin. The precipitation of lignin at low pH, as in our case (pH 2.5), favors the increase of both products. Moreover, the severity of the cooking treatment conditions can also contribute to increase the ASL content in the recovery fraction due to the progressive depolymerization of the lignin with increased cooking time.

Finally, the ash content found in the precipitated lignin was 35.66% at 900 °C. This high amount can be attributed to the high content of salts presented in the sample. Similar and even higher ash contents were found by Dos Santos *et al.* [31] when they precipitated lignin at different pHs (55.8–71.6%).

3.2 Fourier Transform Infrared Spectroscopy Analysis

Figure 1a shows the FTIR spectrum of KL sample. As reported by Boeriu *et al.* [34], lignin presents a broad band at 3424 cm⁻¹, attributed to the hydroxyl groups in phenolic and aliphatic structures, and two bands centered around 2918 and 2849 cm⁻¹, predominantly arising from CH stretching in aromatic methoxyl groups and in methyl and methylene groups of side chains. These bands are less intense for KL than those of original lignin in wood (data not shown), suggesting a decrease in the number of aliphatic methylene and methyl groups during Kraft pulping. In addition, a peak corresponding to the C=O in the unconjugated ketones, carbonyl, and ester groups stretching was observed at 1720 cm⁻¹ [32]. Moreover, the spectrum shows the typical lignin triplet at 1610, 1516 and 1425 cm⁻¹ band due to aromatic ring vibration. The FTIR spectrum also shows a higher intensity of the band assigned to aromatic ring breathing in S unit (1330 cm⁻¹) than in G units (1260 cm⁻¹), typically found in hardwood, and a high intensity band at 1115 cm⁻¹ related to the asymmetric stretching of SO_4 groups due to the formation of salts during lignin precipitation [35, 31], in agreement with the ash content in lignin composition previously discussed.

The KL functionalization with HMDI produces a compound whose FTIR spectrum is shown in Figure 1b. The broad band of hydroxyl groups found at 3424 cm⁻¹ in the unmodified Kraft lignin FTIR disappears almost completely. This is evidence of the reaction between isocyanate and OH groups of lignin.

Secondly, the urethane bands were apparent at 3324 (N-H), 1739 (C=O), and 1574 cm⁻¹ (N-H). Moreover, the intense peak at 2270 cm⁻¹ confirms the presence of free isocyanate groups. Finally, as can be observed in Figure 1c, the reaction between free NCO in the thickener with the OH groups in the fatty acid of the castor oil is also corroborated in the spectrum of the gel-like dispersion, in which the emergence of one band at around 3336 cm⁻¹, assigned to –NH groups, and the disappearance of the free isocyanate peak at 2270 cm⁻¹ can be noticed. Moreover, the inclusion of castor oil is noticed in two characteristic peaks. The first of them at 3007 cm⁻¹ attributed to C=C and the second one at 1746 cm⁻¹ for C=O.

Figure 2 shows the FTIR spectra for a selected gel-like dispersion (GKL2-30), as a function of ageing time (one day, one week and one month). As has been previously discussed, the intensity of the band assigned to free isocyanates (2270 cm⁻¹) is progressively reduced until being almost negligible after one month. On the contrary, a significant amount of free –NCO groups is detectable one day after preparation. This means that the reaction between free isocyanates and hydroxyl groups in such viscous medium is extremely slow, as previously reported for similar biopolyure-thanes [36]. Then, there are some peaks that are well defined one month after preparation (3007, 2918, 2849 and 1746 cm⁻¹). The shape of the band at 3336 cm⁻¹ is modified as a consequence of the progressive reaction between the hydroxyl groups in the fatty acid chain of castor oil and free NCO inserted in the modified lignin, which promotes the appearance of new NH groups in the urethane linkages.
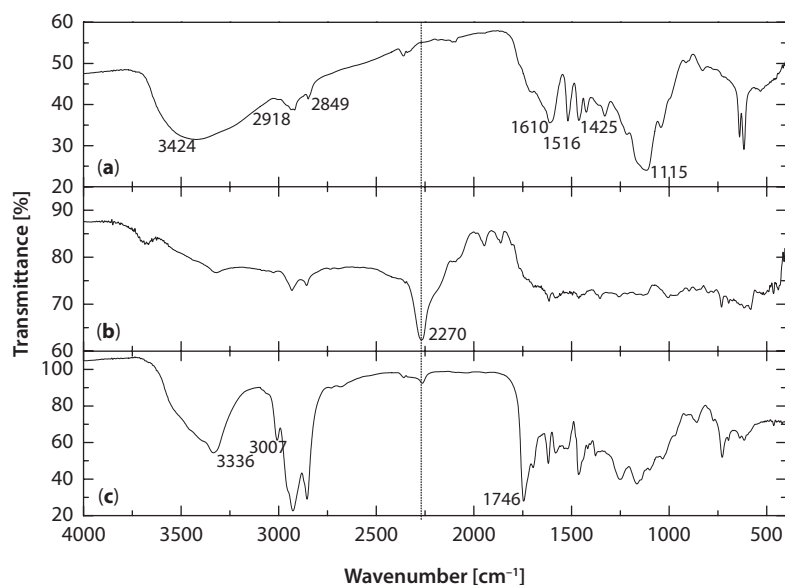
Figure 1 FTIR spectra for (**a**) Kraft lignin, (**b**) KL2 and (**c**) gel-like dispersion GKL2-30.
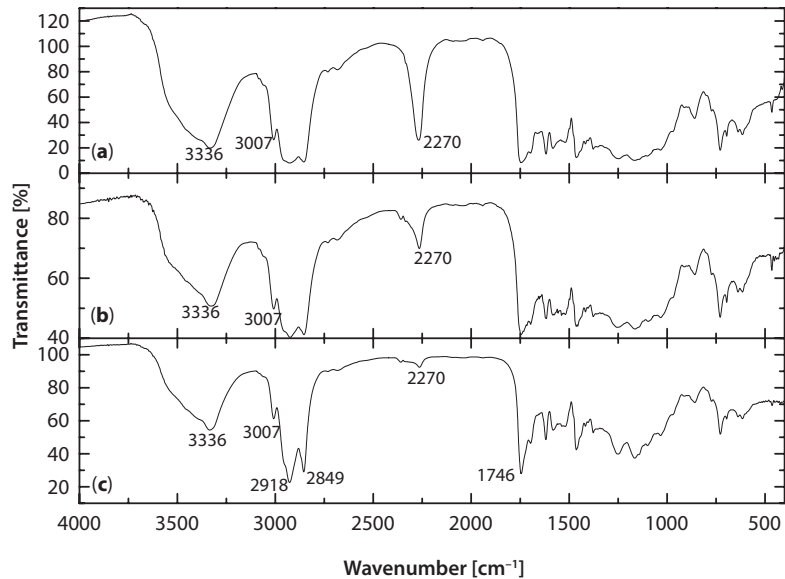
Figure 2 FTIR spectra for gel-like dispersion GKL2-30 as a function of the ageing time: (**a**) one day, (**b**) one week and (**c**) one month after their preparation.
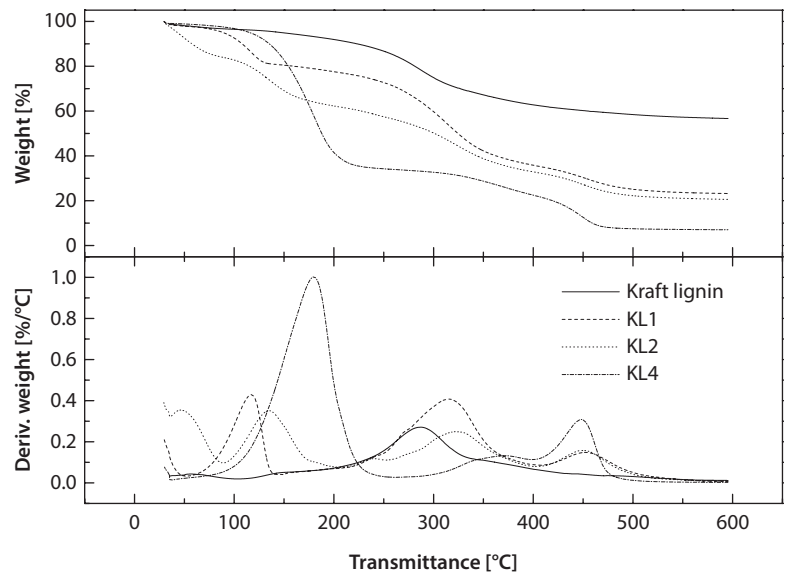
Figure 3 Thermal degradation curves, under inert atmosphere, for Kraft lignin and NCO-functionalized lignins studied.

3.3 Thermogravimetric Analysis

Thermal degradation of KL- and NCO-functionalized lignin compounds was investigated by means of thermogravimetric analysis (TGA). Figure 3 shows TGA curves in the form of weight loss versus temperature and its derivative function for KL and chemically modified lignins as a function of the functionalization degree. The temperature for the onset of thermal decomposition (T_{onset}), the temperature at

which decomposition rate is maximum (T_{max}), final temperature (T_{final}), loss weight at the end of each decomposition step and the percentage of nondegraded residue have been determined from the thermograms of the different samples and collected in Table 3.

As can be observed in Figure 3 and Table 3, thermal degradation of KL, ignoring the weight loss of around 2% due to water evaporation, starts at relatively low temperature (T_{onset} = 138 °C and T_{max} = 150 °C) as a

Table 2 Composition of gel-like dispersion formulations studied.

Thickener agent	Concentration (%, w/w)	Vegetable oil (up to 100 %, w/w)	Gel-like dispersion code
KL1	20	Castor	GKL1-20
KL2	20	Castor	GKL2-20
KL2	30	Castor	GKL2-30
KL4	20	Castor	GKL4-20

Table 3 TGA characteristic parameters for Kraft lignin, NCO-functionalized lignin samples and gel-like dispersions studied.

Sample	T_{onset} (ºC)	T_{max} (ºC)	T_{final} (ºC)	Residue (%)	ΔW (%)
Kraft Lignin	**68/138/248/416**	**58/150/288/348**	**91/195/325/443**	**57**	**2/2/24/15**
HDMI	137	172	178	1	99
KL1	94/262/411	117/316/453	134/361/502	23	17/43/17
KL2	119/293/478	135/322/449	172/371/500	21	32/32/15
KL4	140/339/463	179/371/448	211/396/474	7	65/11/17
GKL1-20	344	378/437	473	4	80/16
GKL2-20	340	374/435	475	2	84/14
GKL2-30	324	367/430	476	1	80/19
GKL4-20	327	371/444	472	0.5	85/14.5

consequence of hydroxyl groups dehydration from benzyl groups [1]. The cleavage of α- and β-aryl-alkyl-ether linkages takes place between 150 and 300 °C. At around 288 °C, aliphatic side chains start splitting off from the aromatic ring while carbon-carbon cleavage between lignin structural units occurs at around 350–443 °C. NCO-functionalized lignin thermal decomposition occurs in several stages, generally three. First, the degradation of HMDI moieties appears in the range of 118–180 °C, which is accountable for the reduction in thermal stability of this type of functionalized thickener [27]. The T_{onset} for this degradation stage takes place at around 94–140 °C, with temperatures for the maximum decomposition rate at around 117–179 °C, depending on the degree of functionalization. The second main thermal event, with temperatures for the maximum decomposition rate at 316–371 °C, is attributed to the degradation of aliphatic side chains and aromatic rings of lignin. Finally, the last stage at 411–463 °C can be associated with carbon-carbon cleavage between lignin structural units and degradation of more rigid polyurethanes due to excessive crosslinking [37]. As shown in Table 3, when the HMDI content in the modified lignin increases, the values of T_{onset}, T_{final} and T_{max} also increase in each stage. Obviously, the modified lignin sample with higher –NCO content (KL4) shows higher weight loss in the first stage (65%) and lower weight loss value (11%) in the second thermal degradation process. Furthermore, the lower amount of residue (7%) was obtained for KL4, whereas it was 57% for KL sample.

Figure 4 shows the thermal decomposition of lignin derivative-based gel-like dispersions. This decomposition takes place in one main single stage with T_{max} of around 367–378 °C, comprising several overlapped degradation events which appear as shoulders of the main peak in the derivative function. Thus, for GKL2-30 and GKL4-20, shoulders at both sides are clearly distinguished, whereas the first shoulder, located at the lower temperatures, is not apparent in GKL1-20 and GKL2-20. These overlapped thermal events comprise the thermal degradation of both NCO-functionalized lignin previously discussed and castor oil, the main component in gel-like dispersions [25]. However, the first degradation stage found in functionalized lignin was not observed in gel-like dispersions, which is indicative of the almost total completion of the reaction between free isocyanates and castor oil. Table 3 shows all TGA characteristic parameters obtained from the thermograms of gel-like dispersions, which generally evidence a higher thermal resistance than that generally exhibited by mineral oil-based lubricating greases [38].
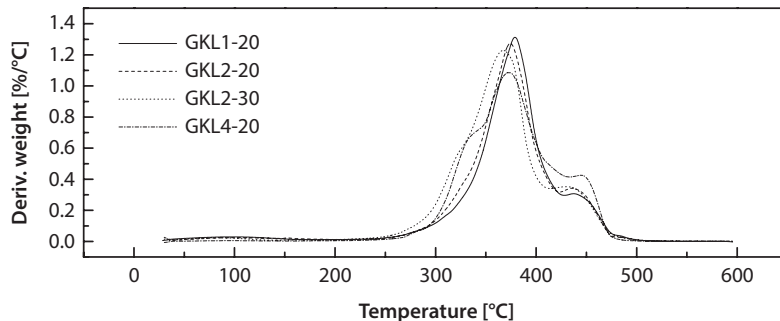
Figure 4 Thermal degradation curves, under inert atmosphere, for gel-like dispersions from NCO-functionalized lignin.
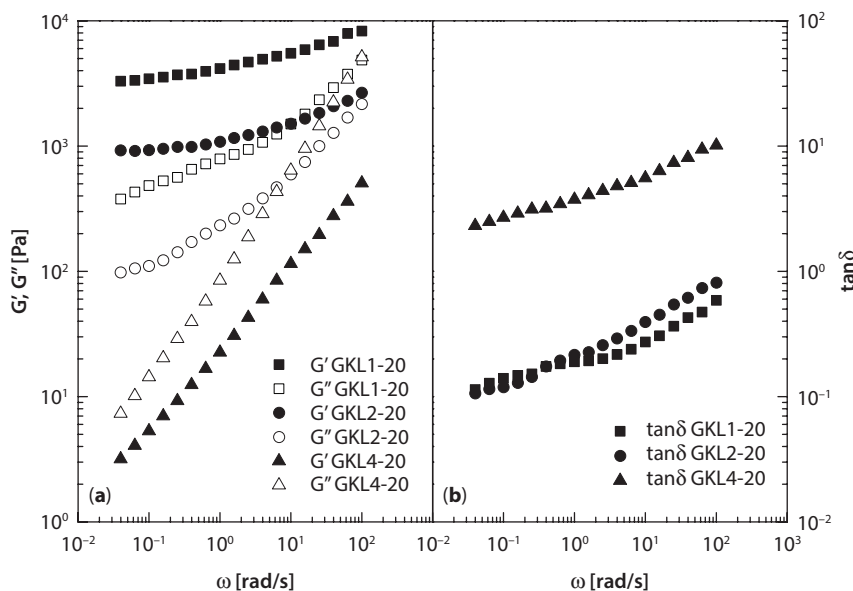
Figure 5 Frequency dependence of (**a**) the storage, G′, and loss, G″, moduli and (**b**) the loss tangent for NCO-functionalized lignin gel-like dispersions in castor oil, as a function of functionalization degree, 1 day after their preparation.

3.4 Rheological Characterization of NCO-Functionalized Lignin Gel-Like Dispersions

Figure 5 shows the SAOS response of NCO-functionalized lignin gel-like dispersions in castor oil, at a concentration of 20% w/w, one day after their preparation, as a function of the HMDI content in the modified lignin. The storage modulus, G″, generally shows higher values than the loss modulus, G″, in the whole frequency range studied, for the gel-like dispersions prepared with lower NCO contents (GKL1-20 and GKL2-20), associated with the plateau region of the mechanical spectrum, followed by the beginning of the transition region. According to Lu *et al.* [39], the gel strength of biopolymer dispersed systems is mainly dependent on the crosslinking density, which

can be analyzed from SAOS measurements attending the G′ and G″ frequency dependence, i.e., the slopes of G′ and G″ versus frequency plots, and the relative elasticity, expressed in terms of the loss tangent (tan δ = G″/G′). Thus, GKL1-20 and GKL2-20 exhibit a gel-like rheological behavior with relatively low slopes of SAOS functions versus frequency plots (Figure 5a). On the contrary, the gel-like dispersion prepared with the highly functionalized lignin (GKL4-20) essentially exhibits a viscous response, with values of G″ higher than G′ in the whole frequency range studied. Moreover, the values of the loss tangent for GKL4-20 are more than one order of magnitude higher than those found for GKL1-20 and GKL2-20 (Figure 5b), thus showing a lower relative elasticity. This result obtained with sample GKL4-20 is in principle unexpected since the higher HMDI excess in lignin functionalization

should extend the plateau region of the mechanical spectrum and reduce the slope of SAOS functions, as a result of the higher degree of crosslinking. However, the slopes of both SAOS functions vs. frequency plots suggest a certain degree of crosslinking among low-molecular-weight compounds, resulting in the typical transition region of the mechanical spectrum [40]. On the other hand, the kinetics of the reaction between free –NCO groups and castor oil triglycerides is relatively slow in such viscous medium, as confirmed in FTIR analysis (see Figure 2), and is highly dependent on the functionalization degree. This fact extremely influences the rheology of these gel-like dispersions, which can dramatically evolve with ageing time. This effect is clearly illustrated in Figure 6, where samples GKL2-20 and GKL4-20 are compared not just after preparation but one month later. As can be observed, whereas the values of SAOS functions slightly increase with time for sample GKL2-20, a dramatic increment was found for GKL4-20, also changing the frequency dependence displayed in Figure 5 to reach the typical gel-like response. This fact corroborates that the chemical interaction between the functionalized lignin and castor oil is mainly responsible for the gel-like behavior. Therefore, considering the comparison included in Figures 5 and 6 for the same concentration by weight (20%), the rheological behavior of these dispersions can be explained as a balance between a quick structuring effect caused by the polymer, favored by higher lignin/HMDI ratios, which yields higher values of the SAOS functions and lower frequency dependence

from the beginning, and the excess of free HMDI, which delays the chemical interaction between the modified lignin and castor oil, probably involving competitive reactions which can produce crosslinking among polymeric chains or among triglycerides.

Regarding thickener concentration, Figure 6 also includes the mechanical spectra of the gel-like dispersion prepared with 30% w/w of NCO-functionalized lignin containing a lignin/HMDI weight ratio of 1:2 (sample GKL2-30). As can be seen, almost two orders of magnitude of both viscoelastic functions can be covered by modifying the thickener concentration between 20% and 30% (w/w). In addition to this, the evolution of viscoelastic functions with frequency slightly depends on lignin concentration. Thus, the lower NCO-functionalized lignin concentration (20%) yields a crossover of both SAOS functions at high frequencies, i.e., the beginning of the transition region (Figure 6a). On the contrary, a well-extended plateau region in the whole frequency range was obtained by increasing thickener concentration up to 30% (w/w), where G′ slightly increases with frequency and G″ displays a clear minimum at low frequencies. This evolution was typically found in other gel-like dispersions of different biopolymers in vegetable oil previously studied [24, 26] and standard lubricating greases [38]. As extensively studied, typical G′ values in lubricating greases of NLGI grade 1–2 range from 10^4 to 10^5 Pa, around one order of magnitude higher than G″ values, depending on processing conditions and compositions [38, 41], as, for instance, achieved with samples
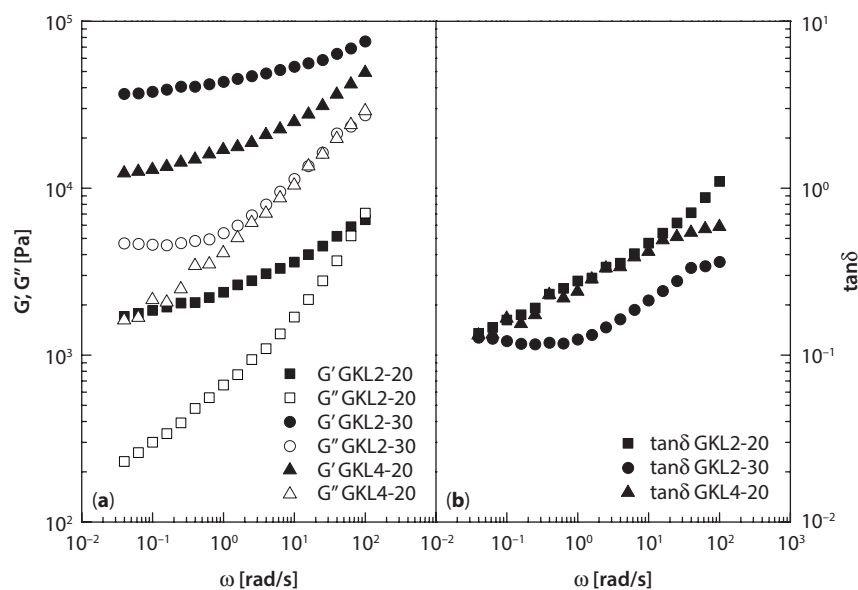
Figure 6 Frequency dependence of (**a**) the storage, G′, and loss moduli, G″, and (**b**) the loss tangent for NCO-functionalized lignin gel-like dispersions in castor oil, as a function of NCO-functionalized lignin concentration, 1 month after their preparation.

GKL2-30 and GKL4-20. Nonetheless, sample GKL4-20 becomes almost a rubber after approximately one month as a consequence of the excessive chemical crosslinking.

In relation to long-term stability, Figure 7 illustrates the influence of ageing time on the storage modulus, at 1 rad/s, for three selected NCO-functionalized lignin gel-like dispersions in castor oil (GKL2-20, GKL2-30 and GKL4-20). As can be seen, the values of G' significantly increase during the first seven days of ageing, slightly increase until one month and then remain almost constant for a long period of time. As

previously discussed, these results can be explained on the basis of the slow reactivity of residual –NCO functional groups in a highly viscous medium [36].

The influence of the temperature on the SAOS functions was also studied for a selected sample prepared using a lignin/HMDI weight ratio of 1:2 and a concentration of 30% w/w (GKL2-30). This sample was selected considering its mechanical spectrum at 25 °C, which is more similar to those found in conventional lithium lubricating greases. As can be observed in Figure 8, the linear viscoelastic functions, G' and G″, generally decrease with temperature in the whole
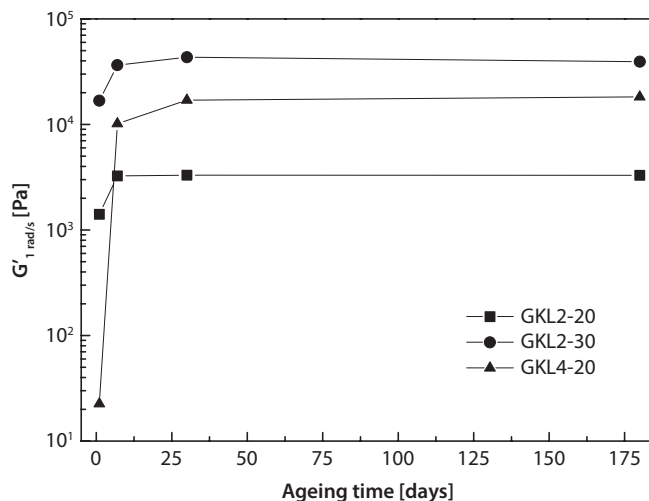
Figure 7 Evolution of the storage modulus, G', at 1 rad/s, with the ageing time for selected NCO-functionalized lignin gel-like dispersions in castor oil.
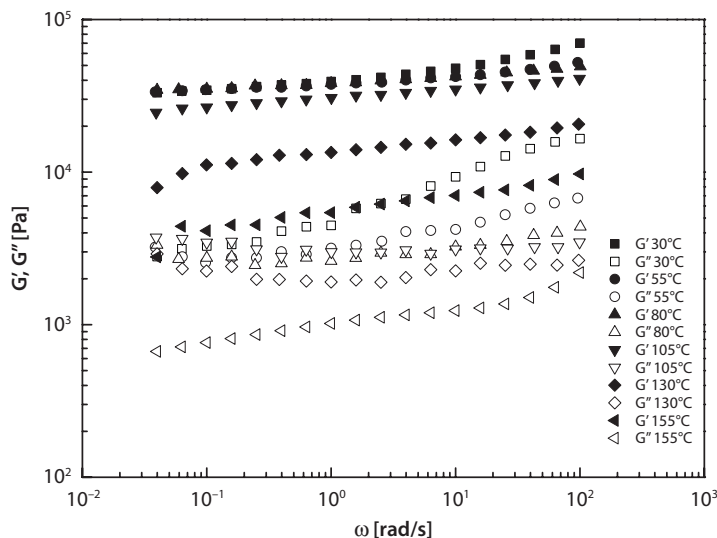
Figure 8 Evolution of the storage and loss moduli with frequency, at different temperatures, for a selected NCO-functionalized lignin gel-like dispersion (GKL2-30).

frequency range studied, much more sharply above 105 °C. G′ frequency dependence is not significantly affected by temperature and G″ is influenced mainly at high frequencies. At temperatures higher than 155 °C, a significant "oil bleeding" is generally observed, which limits the thermo-rheological characterization. The plateau modulus, G_N^0, can be used to quantify the SAOS function-temperature dependence (Figure 9). As mentioned above, a sudden change in the slope of G_N^0 versus $1/T$ plot at around 105 °C was clearly seen, thus indicating a much higher thermal susceptibility of sample studied at temperatures above this critical temperature. This critical temperature matches fairly well with that referred for the softening point of traditional lithium lubricating greases, which is around 110 °C. Two different Arrhenius-type relationships are proposed to describe the evolution of G_N^0 with temperature in both temperature ranges, as previously reported [28, 42]:

$$G_N^o = A \cdot e^{(E_a/R) \cdot (1/T)} \qquad (1)$$

where E_a is a fitting parameter that gives information about the gel-like dispersion thermal dependence, with a physical meaning similar to an activation energy (J mol^{-1}), R is the gas constant (8.314 J mol^{-1} K^{-1}), T is the absolute temperature (K), and A is the pre-exponential factor (Pa). Equation 1 fits the experimental plateau modulus values for the selected sample, in the whole temperature range studied, fairly well ($R^2 > 0.90$, see Figure 9). The activation energy values resulting from this fitting were 1.3 kJ mol^{-1} in the low temperature range and 50 kJ mol^{-1} in the high temperature range. These values are similar to those obtained for standard lithium greases in

the low temperature range (1–2 kJ mol^{-1}) and higher than those reported in the high-temperature range (18–20 kJ mol^{-1}) [42]. However, this thermal dependence is lower than that shown by other biodegradable lubricating greases based on castor oil and lignocellulose pulps from different origins and/or submitted to different crosslinking treatments with hexamethylene diisocyanate [28].

From a rheological point of view, the formulation of new lubricating greases needs the characterization of both linear viscoelastic and viscous flow behaviors. The viscous flow behavior of NCO-functionalized lignin gel-like dispersions seems to be not so significantly affected by the amount of HMDI used to modify the lignin. However, the concentration of thickener used in the formulation affects the viscosity, as can be seen in Figure 10, where viscous flow curves of gel-like dispersions containing a lignin/HMDI weight ratio of 1:1 and 1:2 and concentrations of 20% and 30% w/w have been compared. The power-law model fits the viscous flow behavior of these gel-like dispersions fairly well ($R^2 > 0.99$) in the experimental range of shear rates studied,

$$\eta = k \cdot \dot{\gamma}^{n-1} \qquad (2)$$

where "k" and "n" are the consistency and flow indexes respectively. The values of these fitting parameters are shown in Figure 10. As can be observed, the values of the consistency and flow indexes slightly decrease with the lignin/HMDI weight ratio, the latter one being extremely low, especially for GKL1-20, as typically found in lubricating greases, which have been traditionally considered classical yielding materials. GKL2-30 displays the higher consistency index,
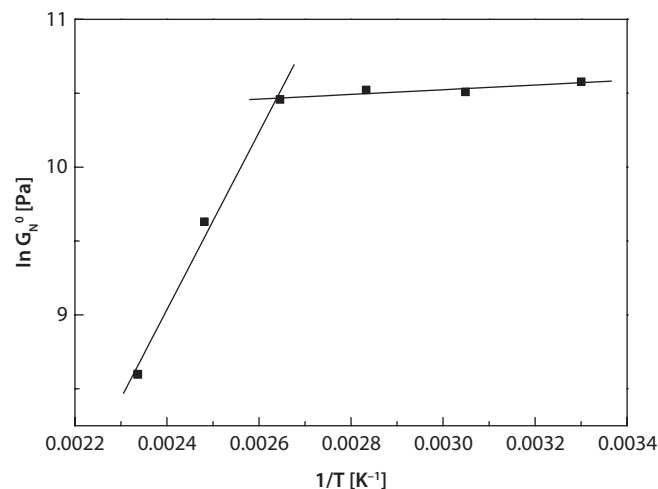
Figure 9 Evolution of the plateau modulus with temperature and Arrhenius' fitting (solid line) for a selected NCO-functionalized lignin gel-like dispersion (GKL2-30).
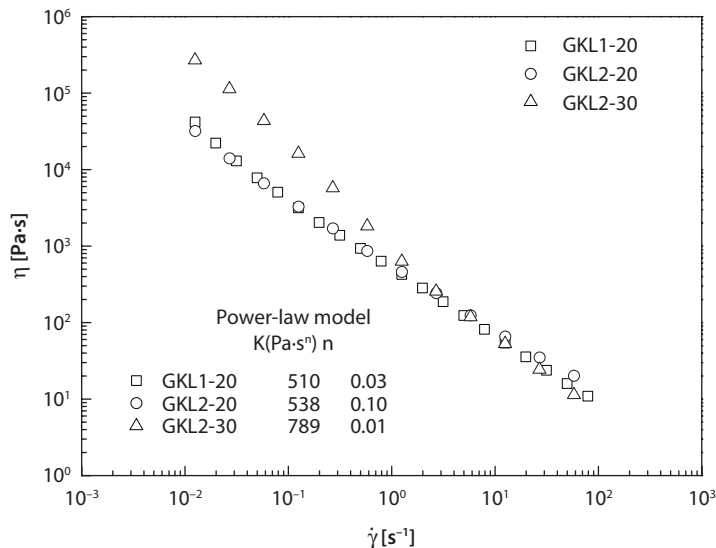
Figure 10 Viscous flow curves for NCO-functionalized lignin gel-like dispersions studied, at 25 °C, as a function of HMDI/lignin weight ratio and concentration.

which may be attributed to the higher thickener concentration.

3.5 AFM Analysis of NCO-Functionalized Lignin Gel-Like Dispersions

Figure 11 shows the microstructure of a selected NCO-functionalized lignin gel-like dispersion (GKL2-20), evaluated by using the AFM technique. The advantage of this technique in contrast to classical electron microscopy observations is that the sample does not need to be modified since the experiments can be carried out under atmospheric pressure. Thus, both scanning (SEM) and transmission (TEM) electron microscopy techniques are vacuum based and the sample must be submitted to either a freezing treatment or oil removal. Appropriate microstructural characterization of conventional lubricating greases and lignocellulose pulp gel-like dispersions were previously reported just by simply heating the sample at a temperature below the dropping point and then cooling down to room temperature in order to obtain a very smooth surface [43]. In this work, the sample was prepared following the same protocol. As can be noticed, the microstructure of this sample is composed of interconnected thin fibers, forming a three-dimensional network, which are distributed in a continuous oil medium. Average fiber thickness and length are around 24–30 nm and 178–230 nm, respectively. These chemically modified lignin dispersions show more densely grouped, thinner and shorter fibers than those found for conventional lubricating
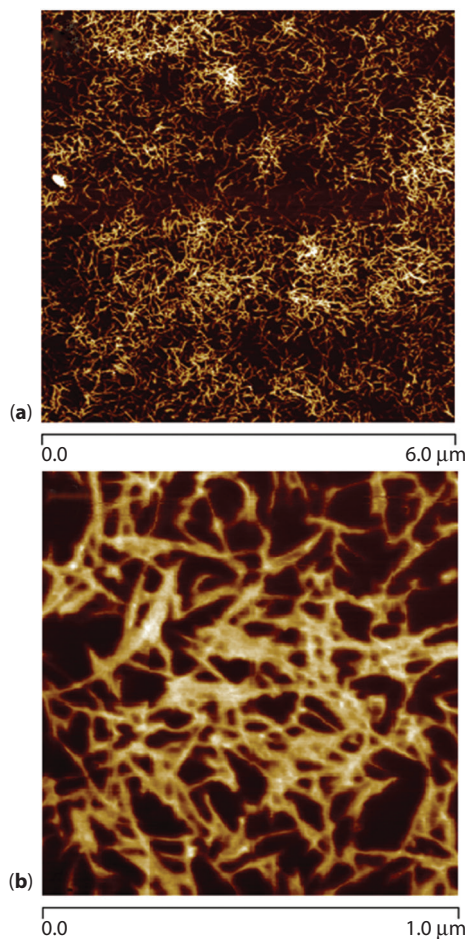
Figure 11 AFM micrographs for selected NCO-functionalized lignin gel-like dispersion (GKL2-20): (**a**) window size 6 μm; (**b**) window size 1 μm.

greases and HMDI-crosslinked lignocellulose pulp gel-like dispersions, previously described [28, 43].

3.6 Lubrication Performance Properties of NCO-Functionalized Lignin Gel-Like Dispersions

The lubrication properties of NCO-functionalized lignin gel-like dispersions studied were evaluated by means of penetration tests and tribological experiments, and the results have been compared with those shown by commercial lithium and calcium lubricating greases. Penetration of standard cone geometries inside a given lubricating grease sample is a common practice in the lubricant industry to determine grease consistency, which is obviously related to the rheological properties. The NLGI grade is a commonly accepted parameter to classify lubricating greases as a function of their consistency obtained as penetration index [30]. Table 4 shows unworked penetration values of gel-like dispersions studied, along with the corresponding NLGI grade, and friction coefficients obtained in the tribological cell. The gel-like dispersion with the higher thickener concentration and lignin/HMDI weight ratio of 1:2 is more viscous (see Figure 10) and therefore shows lower unworked penetration value and higher NLGI grade. Beside this, a decrease of lignin/HMDI weight ratio in the thickener results in a decrease of unworked penetration and higher NLGI grade. On the other hand, all samples studied provide similar friction coefficient values which are lower than those obtained for the commercial lubricating greases under the same tribological conditions. Although friction coefficient depends on operating conditions and wear mechanisms, this is a relevant result since the main purpose of using lubricants in a tribological contact is the reduction of friction as much as possible. In this sense, the model gel-like dispersions studied in this work show a reduction of 16–22% in the friction coefficient with respect to the two standard commercial greases used as references.

4 CONCLUSIONS

This work describes a potential form of industrial valorization of residual Kraft lignin via modification with HMDI and subsequent dispersion in castor oil to obtain gel-like dispersions with suitable and promising properties to be used as biodegradable lubricating greases. Rheological functions of these gel-like dispersions are qualitatively and quantitatively affected by the lignin/ HMDI weight ratio and modified lignin concentration. In most cases, the values of the storage modulus are always higher than those found for the loss modulus in a wide frequency range, displaying the plateau region of the mechanical spectrum which is characteristic of particle gels and lubricating greases among them. The rheological functions evolve with ageing time, up to around one month after preparation, as a consequence of an internal curing process where free isocyanates react with castor oil triglycerides. The effect of the curing process is especially dramatic for the sample containing a lignin/HMDI weight ratio of 1:4, which exhibits a predominant viscous response immediately after preparation and becomes almost a rubber after one month. In particular, the frequency dependence of SAOS functions of 30% modified lignin gel-like dispersion with 1:2 lignin/HMDI weight ratio is very similar to that found for traditional NLGI 2 lithium lubricating greases. In relation to long-term rheological stability, the values of SAOS functions significantly increase during the first seven days of ageing, slightly increase up to one month and then remain almost constant for a long period. The thermo-rheological response evidences a softening temperature of around 105 °C. The unworked penetration values and related NLGI grade is essentially viscosity dependent. An increase in lignin functionalization degree results in a decrease of the unworked penetration for the same concentration. All samples studied provide similar friction coefficient values in a tribological contact, lower than those obtained with standard commercial lubricating greases.

Table 4 Penetration, NLGI and friction coefficient for samples studied.

Sample	Unworked penetration (dmm)	NLGI	Friction coefficient
GKL1-20	330	1	0.086
GKL2-20	287	2	0.083
GKL2-30	198	4	0.089
Lithium-based grease	260	2–3	0.108
Calcium-based grease	279	2	0.107

ACKNOWLEDGMENTS

REFERENCES

1. S. Laurichesse and L. Avérous, Chemical modification of lignins: Towards biobased polymers. *Prog. Polym. Sci.* **39**, 1266–1290 (2014).

2. I.H. Bolker, *Natural and Synthetic Polymers: An Introduction*, Marcel Dekker, New York (1974).

3. A. Tejado, C. Peña, J. Labidi, J.M. Echevarria, and I. Mondragon, Physico-chemical characterization of lignins from different sources for use in phenol-formaldehyde resin synthesis. *Bioresour Technol*. **98**, 1655–1663 (2007).

4. X. Du, J. Li, and M.E. Lindström, Modification of industrial softwood Kraft lignin using Mannich reaction with and without phenolation pretreatment. *Ind. Crops Prod*. **52**, 729–735 (2014).

5. C. Bonini, M. D'Auria, L. Emanuele, R. Ferri, R. Pucciatiello, and A.R. Sabia, Polyurethanes and polyesters from lignin. *J. Appl. Polym. Sci.* **98**(3), 1451–1456 (2005).

6. D.V. Evtuguin, J.P. Andreolety, and A. Gandini, Polyurethanes based on oxygen-organosolv lignin. *Eur. Polym. J.* **34**(8), 1163–1169 (1998).

7. H. Hatakeyama and T. Hatakeyama, Thermal Properties of isolated and in situ lignin, in *Lignin and Lignans: Advances in Chemistry*, C. Heitner, D. Dimmel, and J. Schmidt (Eds.), pp. 301–319, CRC Press, Boca Raton (2011).

8. T. Hatakeyama, Y. Izuta, S. Hirose, and H. Hatakeyama, Phase transitions of lignin-based polycaprolactones and their polyurethane derivatives. *Polymer* **43**(4), 1177–1182 (2002).

9. J. Bernardini, P. Cinelli, I. Anguillesi, M.B. Coltelli, and A. Lazzeri, Flexible polyurethane foams green production employing lignin or oxypropylated lignin. *Eur. Polym. J.* **64**, 147–156 (2015).

10. C.Q. Zhang, H.C. Wu, and M.R. Kessler, High biocontent polyurethane composites with urethane modified lignin as filler. *Polymer* **69**, 52–57 (2015).

11. D. Feldman, M. Lacasse, and L.M. Beznaczuk, Lignin-polymer systems and some applications. *Prog. Polym. Sci.* **12**, 271–276 (1986).

12. P.C. Mileo, M.F. Oliveria, S.M. Luz, G.J.M. Rocha, and A.R. Gonçalves, Thermal and Chemicals characterization of sugarcane bagasse cellulose/lignin-reinforced composites. *Polym. Bull*. **73**, 3163–3174 (2016).

13. A. Lee and Y.L. Deng, Green polyurethane from lignin and soybean oil through non-isocyanate reactions. *Eur. Polym. J*. **63**, 67–73 (2015).

14. X.G. Luo, A. Mohanty, and M. Misra, Lignin as a reactive reinforcing filler for water-blow rigid biofoam composites from soy oil-based polyurethane. *Ind. Crops Prod*. **47**, 13–19 (2013).

15. L.B. Tavares, C.V. Boas, G.R. Schleder, S.M. Nacas, D.S. Rosa, and D.J. Santos, Bio-based polyurethane prepared from Kraft lignin and modified castor oil. *Express Polym. Lett*. **11**, 927–940 (2016).

16. J.W. Bartz, Lubricants and the environment. *Tribol. Int*. **31**, 35–47 (1998).

17. C.W. Lea, European development of lubricants derived from renewable resources. *Ind. Lubr. Tribol*. **54**, 268–274 (2002).

18. S. Boyde, Green lubricants. Environmental benefits and impacts of lubrication. *Green Chem*. **4**, 293–307 (2002).

19. F.S. Guner, Y. Yagci, and A.T. Erciyes, Polymers from triglyceride oils. *Prog. Polym. Sci*. **31**, 633–670 (2006).

20. L.A. Quinchia, M.A. Delgado, J.M. Franco, H.A. Spikes, and C. Gallegos, Low-temperature flow behaviour of vegetable oil-based lubricants. *Ind. Crops Prod*. **37**, 383–388 (2012).

21. S. Asadauskas, J.M. Perez, and J.L. Duda, Lubrication properties of castor oil. Potential basestock for biodegradable lubricants. *Lubr. Eng*. **53**, 35–41 (1997).

22. S.Z. Erhan, B.K. Sharma, and J.M. Perez, Oxidation and low temperature stability of vegetable oil-based lubricants. *Ind. Crops Prod.* **24**, 292–299 (2006).

23. R. Sánchez, J.M. Franco, M.A. Delgado, C. Valencia, and C. Gallegos, Effect of thermo-mechanical processing on the rheology of oleogels potentially applicable as biodegradable lubricating greases. *Chem. Eng. Res. Des*. **86**, 1073–1082 (2008).

24. R. Sánchez, J.M. Franco, M.A. Delgado, C. Valencia, and C. Gallegos, Thermal and mechanical characterization of cellulosic derivatives-based oleogels potencially applicable as bio-lubricating grease: Influence of ethyl cellulose molecular weight. *Carbohydr. Polym*. **83**, 151–158 (2011).

25. N. Nuñez, J.E. Martín-Alfonso, M.E. Eugenio, C. Valencia, M.J. Díaz, and J.M. Franco, Preparation and characterization of gel-like dispersions based on cellulosic pulps and castor oil for lubricating applications. *Ind. Eng. Chem. Res*. **50**, 5618–5627 (2011).

26. N. Nuñez, J.E. Martín-Alfonso, C. Valencia, M.C. Sánchez, and J.M. Franco, Rheology of new green lubricating grease formulations containing cellulose pulp and its methylated derivative as thickener agents. *Ind. Crops Prod.* **37**, 500–507 (2012).

27. R. Gallego, J.F. Arteaga, C. Valencia, and J.M. Franco, Rheology and thermal degradation of isocyanate-functionalized methyl cellulose-based oleogels. *Carbohydr. Polym*. **98**, 152–160 (2013).

28. R. Gallego, J.F. Arteaga, C. Valencia, M.J. Díaz, and J.M. Franco, Gel-like dispersions of HMDI-cross-linked lignocellulosic materials in castor oil: Toward completely renewable lubricating grease formulations. *ACS Sus. Chem. Eng*. **3**, 2130–2141 (2015).

29. C. Balan and J.M. Franco, Influence of the geometry on the transient and steady flow of lubricating greases. *Tribol. Trans*. **44**, 53–58 (2001).

30. National Lubricating Grease Institute, *NLGI: Lubricating Greases Guide*, NLGI, Kansas (2006).

31. P.S.B. Dos Santos, X. Erdocia, D.A. Gatto, and J. Labidi, Characterization of Kraft lignin separated by gradient acid precipitation. *Ind. Crops Prod.* **55**, 149–154 (2014).

32. M. Alekhina, O. Ershova, A. Ebert, S. Heikkinen, and H. Sixta, Softwood kraft lignin for value-added applications: Fractionation and structural characterization. *Ind. Crops Prod.* **66**, 220–228 (2015).

33. S. Yasuda, K. Fukushima, and A. Kakehi, Formation and chemical structures of acid-soluble lignin I: Sulphuric acid treatment, time and acid-soluble lignin content of hardwood. *J. Wood Sci.* **47**, 69–72 (2001).

34. C.G. Boeriu, D. Bravo, R.J.A. Gosselink, and J.E.G. Van Dam, Characterization of structure-dependent functional properties of lignin with infrared spectroscopy. *Ind. Crops Prod.* **20**, 205–218 (2004).

35. D. Ibarra, M.I. Chávez, J. Rencoret, J.C. Del Río, A. Gutiérrez, J. Romero. S. Camarero, M.J. Martínez, J. Jiménez-Barbero, and A.T. Martínez, Lignin modification during Eucalyptus globulus kraft pulping followed by totally chlorine-free bleaching: A two-dimensional nuclear magnetic resonance, Fourier transform infrared, and pyrolysis-gas chromatography/mass spectrometry study. *J. Agric. Food Chem.* **55**, 3477–3490 (2007).

36. A.M. Borrero-López, C. Valencia, and J.M. Franco, Rheology of lignin-based chemical oleogels prepared using diisocyanate crosslinkers: Effect of the diisocyanate and curing kinetics. *Eur. Polym. J.* **89**, 311–323 (2017).

37. C.V. Mythili, A. Malar Retna, and S. Gopalakrishnan, Synthesis, mechanical, thermal and chemical properties of polyurethanes based on cardanol. *Bull. Mater. Sci.* **27**, 235–241 (2004).

38. J.E. Martín-Alfonso, C. Valencia, M.C. Sánchez, J.M. Franco, and C. Gallegos, Rheological modification of lubricating greases with recycled polymers from different plastic waste. *Ind. Eng. Chem. Res.* **48**, 4136–4144 (2009).

39. L. Lu, X. Liu, and Z. Tsong, Critical exponents for sol-gel transition in aqueous alginate solutions induced by cupric cations. *Carbohydr. Polym.* **65**, 544–551 (2006).

40. J.D. Ferry, *Viscoelastic Properties of Polymers*, 3rd ed., John Wiley & Sons, New York (1980).

41. J.M. Franco, M.A. Delgado, C. Valencia, M.C. Sánchez, and C. Gallegos, Mixing rheometry for studying the manufacture of lubricating greases. *Chem. Eng. Sci.* **60**, 2409–2418 (2005).

42. M.A. Delgado, C. Valencia, M.C. Sanchez, J.M. Franco, and C. Gallegos, Thermorheological behaviour of a lithium lubricating grease. *Tribol. Lett.* **23**, 47–53 (2006).

43. C. Roman, C. Valencia, and J.M. Franco, AFM and SEM assessment of lubricating grease microstructures: Influence of sample preparation protocol, frictional working conditions and composition. *Tribol. Lett.* **63**(20), 1–12 (2016).